

Although the experimental determination of C_f in the region near the step is suspect, the discrepancy between the calculated and measured C_f well downstream of the step need further investigation. Available experimental results appear to suggest that the relaxation length downstream of either a step up or step down in wall injection is well in excess of $35\delta_0$ when the relaxation of the turbulence structure is also taken into account.

References

- ¹Jeromin, L.O.F., "The Status of Research in Turbulent Boundary Layers with Fluid Injection," *Progress in Aeronautical Sciences*, Vol. 10, Pergamon Press, 1970, pp. 55-189.
- ²Simpson, R.L., "Characteristics of Turbulent Boundary Layers at Low Reynolds Numbers with and without Transpiration," *Journal of Fluid Mechanics*, Vol. 42, July 1970, pp. 769-802.
- ³Coles, D., "A Survey of Data for Turbulent Boundary Layers with Mass Transfer," AGARD Conference Proceedings No. 93, *Turbulent Shear Flows*, 1972, pp. (25-1)-(25-13).
- ⁴McQuaid, J., "The Calculation of Turbulent Boundary Layers with Injection," ARC R and M 3542, Jan. 1967, Aeronautical Research Council, London.
- ⁵McQuaid, J., "Experiments on Incompressible Turbulent Boundary Layers with Distributed Injection," R and M 3549, Jan. 1967, Aeronautical Research Council, London.
- ⁶Levitch, R.N., "The Effect of the Discontinuation of Injection on the Transpired Turbulent Boundary Layer," Sc.D. thesis, 1966, Dept. of Technical Engineering, MIT, Cambridge, Mass.
- ⁷Simpson, R.L., "The Effect of a Discontinuity in Wall Blowing on the Turbulent Incompressible Boundary Layer," *International Journal of Heat Mass Transfer*, Vol. 14, Dec. 1971, pp. 2083-2097.
- ⁸Bradshaw, P., Ferriss, D.H., and Atwell, N.P., "Calculation of Boundary-Layer Development Using the Turbulent Energy Equation," *Journal of Fluid Mechanics*, Vol. 28, May 1967, pp. 593-616.
- ⁹Antonia, R.A. and Beck, R.E., "Turbulent Boundary Layers with Wall Injection," Charles Kolling Research Laboratory Tech. Note, F-69, June 1974, Dept. of Mechanical Engineering, University of Sydney, Sydney, Australia.
- ¹⁰Nayak, U.S.L., "Turbulence Intensity and Boundary-Layer Heat Transfer with Uniform Suction or Injection," Ph.D. thesis, Oct. 1970, Dept. of Mechanical Engineering, Monash University, Melbourne, Australia.
- ¹¹Woodridge, C.E. and Muzzy, R.J., "Boundary-Layer Turbulence Measurements with Mass Addition and Combustion," *AIAA Journal*, Vol. 11, Nov. 1966, pp. 2009-2016.
- ¹²Antonia, R.A. and Luxton, R.E., "The Response of a Turbulent Boundary Layer to a Step Change in Surface Roughness: Part 2, Rough to Smooth," *Journal of Fluid Mechanics*, Vol. 53, June 1972, pp. 737-757.
- ¹³Tani, I., "Review of Some Experimental Results on the Response of a Turbulent Boundary Layer to Sudden Perturbations," *Proceedings, Computations of Turbulent Boundary Layers*, AFOSR-IFP-Standard Conference, Vol. 1, Aug. 1968, pp. 483-494.
- ¹⁴Lili, T. and Michel, R., "Couche Limite Turbulente avec Injection a la paroi d'un Meme Gas ou d'un Gas Etranger," AGARD Conference Proceedings No. 93, *Turbulent Shear Flows*, 1972, pp. (24-1)-(24-10).
- ¹⁵Chan, Y.Y., "Computations of Incompressible Boundary Layer with Suction and Injection," *CASI Transactions*, Vol. 4, Sept. 1971, pp. 108-115.

Transient Conduction in a Finite Slab with Variable Thermal Conductivity

K. Mastanaiah* and A.E. Muthunayagam†
Vikram Sarabhai Space Center, Trivandrum, India

Nomenclature

- A_o = $B_1\delta/(2+B_1\delta)$
 b = slab thickness
 B_1 = Biot number = hb/k_o , nondimensional
 h = heat transfer coefficient

Received December 3, 1974.

Index categories: Solid and Hybrid Rocket Engines; Heat Conduction.

*Engineer, Propulsion Engineering Division.

†Head, Propulsion Engineering Division. Member AIAA.

- C_p = specific heat
 $k(\theta)$ = $k_o(1+\beta\theta)$
 k_o = reference thermal conductivity at $T=T_o$
 $K(\theta)$ = $k(\theta)/k_o$
 t = nondimensional time = $\alpha_o\tau/b^2$
 t_δ = value of t at $\delta=1$ for linear case
 T = temperature
 T_g = driving gas temperature
 x = space coordinate
 z = $\eta/[2\sqrt{t}]$, dimensionless
 α_o = reference thermal diffusivity, $k_o/(\rho C_p)$
 β = constant (thermal conductivity coefficient)
 δ = penetration depth
 λ = constant adjustable parameter
 ρ = density
 τ = time
 η = b/x , nondimensional
 ψ = initial constant property solution
 Θ = nondimensional temperature = $(T-T_o)/(T_g-T_o)$

Subscripts

- $()_x$ = partial derivative with respect to x
 $()_t$ = partial derivative with respect to t
 $()_\eta$ = partial derivative with respect to η

I. Introduction

THERMAL design of heat sink rocket nozzles requires the transient temperature distribution in the finite wall subjected to Newtonian heating at the exposed surface and negligible heat loss from the outer. Because of the high temperature range involved and considerable variation of thermal conductivity with temperature for the commonly employed materials, the customary assumption of constant average property can lead to significant inaccuracies in the desired wall thickness. It is therefore imperative that the thermal conductivity variation is invariably taken into account in the analysis.

Unfortunately no exact solution is possible for this problem, owing to the nonlinearity of the differential equation. To the authors' knowledge, even an approximate solution has not yet been reported in the literature. Moreover, the determination of thermal conductivity over wide temperature range of the present-day materials employed in the space program is relatively difficult and exhaustive by the conventional methods, but is best accomplished by the method of "nonlinear estimation"¹ which is gaining an increasing role in engineering design. Numerical method, if employed for this parameter estimation program, will demand considerable computer time and may not always justify its use.

It is the purpose of this Note to develop therefore a simple closed-form approximate solution that will be useful for the thermal design of rocket nozzles following the nonlinear parameter estimation. Linear variation of thermal conductivity with temperature is assumed here.

II. Analysis

A. Semi-Infinite Domain ($t \leq t_\delta$)

The equations to be solved are

$$\Theta_t = (K(\Theta)\Theta_\eta)_\eta; \quad 0 \leq \eta \leq 1, \quad t > 0 \quad (1)$$

$$\theta_\eta(o, t) = B_1[\theta(o, t) - 1] \quad (2)$$

$$\theta(\delta, t) = 0 \quad (3)$$

$$\theta(\eta, o) = 0 \quad (4)$$

We now seek to find the solution of Eqs. (1-4) by the method of "optimal linearization," recently applied by Vujanovic² for heat transfer problems. The initial solutions $\theta = \psi$ for the constant conductivity case are obtained from Ref. 3, using integral methods with parabolic profile assumed

for temperatures. The details are not however presented here, and for the basic principle of the linearization method, Ref. 2 may be consulted.

The final solution is

$$\theta(\eta, t) = [B_2 / (2 + B_2)] [1 - 2(\eta/\delta) + \eta^2/\delta^2] \quad (5)$$

where

$$6t(I + \beta) = \delta^2/2 + 2\delta/B_2 - 4/B_2^2 \times n[(2 + B_2\delta)/2] \quad (6)$$

$$B_2 = B_1/\lambda_{\text{opt}} \quad (7)$$

$$\lambda_{\text{opt}} = I + \beta \int_0^t A_3^3/\delta^3 dt / \int_0^t A_2^2/\delta^3 dt \quad (8)$$

$$A_0 = B_1\delta / (2 + B_1\delta) \quad (9)$$

For the special case of the constant wall temperature ($B_1 \rightarrow \infty$), the solution will be reduced to

$$\theta(z) = [1 - z/\sqrt{3(I + \beta)}]^2$$

B. Finite Domain ($t > t_\delta$)

Here the boundary condition on the outer surface will be

$$\theta_\eta(I, t) = 0 \quad (10)$$

instead of Eq. (3) which applies for the semi-infinite case. The initial solution is taken from Ref. 3 and optimal linearization is once again carried out for the finite domain.

The resulting solution for the nonlinear problem is

$$\begin{aligned} \theta(\eta, t) = & 1 - [2/(2 + B_2)] (I + B_2\eta - B_2\eta^2/2) \\ & \times \exp \{ [-3B_2/(3 + B_2)] \lambda_{\text{opt}}(t - t_\delta) \} \end{aligned} \quad (11)$$

where

$$B_2 = B_1/\lambda_{\text{opt}} \quad (12)$$

$$\lambda_{\text{opt}} = I + \beta - 4\beta/[3(2 + B_1)] \times [(E^3 - 1)/(E^2 - 1)] \quad (13)$$

$$E = \exp \{ [-3B_1/(3 + B_1)] (t - t_\delta) \} \quad (14)$$

Note that

$$\lim_{t \rightarrow t_\delta} \{ (E^3 - 1)/(E^2 - 1) \} = 3/2 \quad (15)$$

III. Results and Comparisons

Figure 1 shows the temperature distributions in a finite slab with $B_1 = 1$ at $t = 2t_\delta$, $6t_\delta$, and $15t_\delta$ for $\beta = +0.5$ and -0.5 . It is interesting to observe that the intersection point of the two

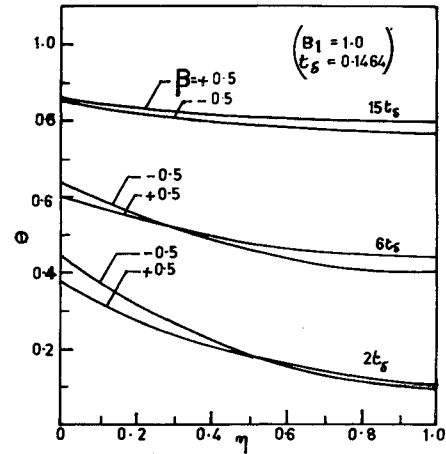


Fig. 1 Temperatures in a finite slab with variable conductivity.

curves moves towards left with increasing t . For sufficiently large t , temperatures for $\beta = +0.5$ are higher than those for $\beta = -0.5$ throughout the slab. This latter trend is well known for the special case of $B_1 \rightarrow \infty$.

Since no exact solution is available in the case of a finite slab, the present solution is compared with finite difference solution in Table 1. In the numerical solution, which uses two time level Crank-Nicholson implicit procedure, Taylor's Forward Projection Method is employed to take into account the nonlinearities for achieving unconditional stability. Fifty space intervals and a time interval of 0.1 sec are taken to insure convergence of solution. Table 1 reveals that the maximum deviation in the two solutions is about 8% at $t = 2t_\delta$ and decreases to about 3% at $t = 6t_\delta$. This suggests that the present solution is in good agreement with the numerical solution.

IV. Nonlinear Estimation

Using the present solution, nonlinear estimation of thermal conductivity variation of M.S. is carried out in conjunction with the experimental data of outer surface temperatures of M.S. used for nozzle divergent in a rocket motor static test. Insulated chromel/alumel thermocouples of 30 gage were used for measuring the temperature. Variable heat transfer coefficient is incorporated in the program. The least-squares minimization of the difference between the theoretical and the experimental system response is accomplished by an extremely simple and very effective optimization procedure⁴ developed recently, which uses direct search and systematic reduction of the size of the search region with the help of random number generation. The optimal values thus obtained for the parameters k_o and β are 30.8 ($W/m \cdot ^\circ K$) and -0.63 , respectively. Comparison of the theoretical response with these values and the experimental response has been found to be satisfactory for engineering design.

Table 1 Comparison of optimal linearization solution with finite difference solution for a finite slab ($B_1 = 1.0$ and $t_\delta = 0.1414$)

t	$2t_\delta$				$6t_\delta$				$15t_\delta$			
	$\beta = -0.5$		$\beta = +0.5$		$\beta = -0.5$		$\beta = +0.5$		$\beta = -0.5$		$\beta = +0.5$	
η	OLS ^a	FDS ^b	ϵ^c	OLS	FDS	ϵ^c	OLS	FDS	ϵ^c	OLS	FDS	ϵ^c
0	0.441	0.429	+2.8	0.373	0.395	-5.58	0.636	0.644	-1.24	0.600	0.610	-1.67
0.2	0.318	0.302	+5.3	0.277	0.300	-7.66	0.551	0.550	+1.82	0.542	0.554	-2.17
0.4	0.221	0.210	+5.25	0.203	0.221	-8.15	0.485	0.480	+1.04	0.496	0.509	-2.56
0.6	0.153	0.147	+4.8	0.150	0.162	-7.40	0.438	0.430	+1.86	0.464	0.474	-2.12
0.8	0.112	0.111	+0.9	0.118	0.126	-6.35	0.409	0.400	+2.25	0.444	0.453	-1.99
1.0	0.099	0.099	0.00	0.108	0.113	-4.43	0.400	0.390	+3.34	0.438	0.446	-1.79

^aOLS = optimal linearization solution (present). ^bFDS = finite difference solution. ^c ϵ = percent error, $\{ (OLS - FDS) / FDS \} \times 100$.

References

- ¹Clark, B.L., "A Parametric Study of the Transient Ablation of Teflon," *Transactions of the ASME, Ser. C: Journal of Heat Transfer*, Vol. 94, Nov. 1972, pp. 347-354.
- ²Vujanovic, B., "Application of Optimal Linearization Method to the Heat Transfer Problem," *International Journal of Heat and Mass Transfer*, Vol. 16, June 1973, pp. 1111-1117.
- ³Mastanaiah, K., "Approximate Solution of Transient Temperature Distribution in a Two-Layer Composite Slab," Internal Rept. SSTC/PSN:TP:1/72, April 1972, VSSC, Trivandrum, India.
- ⁴Jaakola, T.H. and Luus, R., "Optimization of Direct Search and Systematic Reduction of the size of Search Region," *AIChE Journal*, Vol. 19, July 1973, pp. 760-766.

Experimental Verification of Turbulent Skin Friction Reduction with Compliant Walls

Leonard M. Weinstein* and Michael C. Fischer†
NASA Langley Research Center, Hampton, Va.

and

Robert L. Ash‡
Old Dominion University, Norfolk, Va.

Nomenclature

a	= nondimensional amplitude parameter
C_f	= local skin friction coefficient
E	= Young's modulus
f_{vib}	= membrane fundamental vibration frequency
F_{peak}	= peak power frequency in turbulent spectra
L	= length
M_∞	= freestream Mach number
n	= power law exponent
P_t	= tunnel total pressure
q	= dynamic pressure
\dot{q}	= heating rate
R_x	= Reynolds number based on x
T_x	= membrane tension in x direction
T_z	= membrane tension in z direction
t	= material thickness
u	= velocity
w	= width
x	= distance in freestream flow direction from virtual origin
y	= distance perpendicular to model surface
z	= distance along model surface perpendicular to freestream flow direction
δ	= boundary-layer thickness
ρ	= density
τ	= shearing stress

Subscripts

rigid	= referred to rigid condition
ω	= referred to wall condition
∞	= referred to freestream condition

Superscripts

—	= time average value
'	= instantaneous value

Received December 11, 1974.

Index categories: Aircraft Structural Materials; Boundary Layers and Convective Heat Transfer—Turbulent; Subsonic and Transonic Flow.

*Aerospace Engineer, Applied Fluid Mechanics Section, High-Speed Aerodynamics Division.

†Special Assistant, Viscous Drag Reduction, Fluid Mechanics Branch, High-Speed Aerodynamics Division.

‡Associate Professor, School of Engineering.

BOUNDARY-LAYER skin friction drag on subsonic and supersonic aircraft accounts for approximately 50% and 40% respectively, of the total vehicle drag. Laminar (low skin friction) flow exists only near the leading-edge surfaces on typical transport aircraft, so that turbulent boundary-layer (high skin friction) flow is dominant on the vehicle. Since for subsonic jet transports, approximately half of the power required for cruise is necessary to overcome the skin friction drag, the potential savings in fuel, or gain in payload or range from even a moderate skin friction drag reduction, merits a re-evaluation of methods for reducing skin friction drag.

Kramer^{1,2} is credited with the original idea of drag reduction by compliant surfaces, based on his observation of dolphins swimming in water. Kramer's experiments showed a drag reduction of approximately 50% for a towed compliant coated cylinder; however, these results are questionable.³ A survey of both theoretical and experimental investigations of the compliant wall effect is given by Fischer and Ash.³

Total skin friction drag reductions of up to 50% have been reported by Blick and his co-workers⁴ (see Ref. 3 for the numerous other investigations reported by Blick) in their studies of low-speed turbulent boundary-layer air flow over compliant surfaces. More recently, Mattout⁵ conducted tests in water with passive and active (mechanically driven) compliant wall membranes and reported drag reductions of up to 20%. Tests recently completed by McAlister and Wynn⁶ attempted to duplicate Blick's studies; however, they found no drag reduction.

Preliminary compliant wall test results obtained in the Low Turbulence Pressure Tunnel (LTPT) at Langley Research Center have shown promising results. Test conditions for this investigation covered a velocity range of 30-90 m/sec (P_t from 1.01×10^5 - 8.11×10^5 N/m²) and Reynolds number range of 7.4×10^6 - 106×10^6 based on a calculated virtual origin 3.96 m ahead of the survey station. A rigid surface for reference comparison, as well as various compliant wall surfaces, 46.7 cm wide and 127 cm long, were flush mounted on the side wall of the tunnel. Hot wire mean velocity and Reynolds stress data were obtained at one survey station 12.7 cm upstream from the rear of each surface. Limitations in the survey mechanism travel prevented traversing to the boundary-layer edge, but boundary-layer thicknesses of 2.54-7.62 cm were deduced from velocity power law profile fits to the measured data.

All of the compliant surfaces tested except one consisted of 0.64 cm thick polyurethane foam with various surface coverings. Compliant surface skins consisted of 0.0025 cm thick mylar, stretched under tension and area (complete surface) bonded or longitudinally strip bounded with silicone rubber adhesive to the foam and in one case to the rigid surface. Other compliant surfaces consisted of smooth silicone rubber sheets area bonded to the foam. A tension of approximately 1.75 N/cm was applied to the mylar membranes prior to testing, but membrane "bowing" during testing due to a slight differential pressure probably increased the tension and produced visible air gaps in unbounded regions. Two 0.64 cm nominally thick foam substrates were used: 39 pores/cm (PPC) polyurethane foam and compressed 35 PPC polyurethane foam.

Mean velocity and fluctuating survey data were obtained with a single slanted hot wire, which was rotated to measure $\bar{u}'v'$.⁷ Since a single wire was used, matching two different wires was not required. The wire was inclined at approximately 45° with the plane of the wire aligned with the flow and perpendicular to the surface. The wire was used in two positions rotated 180° apart. Absolute measurements of Reynolds stress require angle-of-attack calibration of the probe. However, since these calibrations were not available, the present measurements were ratioed to values obtained on the reference (rigid) plate. The present relative Reynolds stress measurements are believed to be accurate within $\pm 5\%$.

The most effective compliant wall was the 0.0025 cm thick mylar membrane stretched under tension and area bonded to